Effects of Reynolds number on leading-edge vortex formation dynamics and stability in revolving wings

Long Chen[1, *], Luyao Wang[1], Chao Zhou[2], Jianghao Wu[2], and Bo Cheng[3]

[1] *College of Sciences, Northeastern University, Shenyang 110819, People's Republic of China*

[2] *School of Transportation Science and Engineering, Beihang University, Beijing 100191, People's Republic of China*

[3] *Department of Mechanical Engineering, Pennsylvania State University, University Park, Pennsylvania 16801, United States*

[*] *Corresponding author: chenlong@mail.neu.edu.cn*

Supplementary material

The accuracy of the quantitative analysis in our research can be proved by the following verification on the balance of Eq. 2.9 (Fig. S1). The total convection, tilting and stretching, and diffusion in the radial direction within the LEV region at *Re*=1500 are integrated, together with their summation (*Net*). Note that the radial component of planetary vortex tilting (PVT_r) is included in the total vortex tilting and stretching (*T*). As shown in Fig. S1a and S1b, the total convection (*C*) and tilting and stretching (*T*) experience an approximately inversed trend within the stable LEV region (λ=4-6), except for a slight difference in their magnitudes. Moreover, the vorticity diffusion (*D*) at *Re*=1500 is not comparable to *C* and *T* (Fig. S1c), thus leading to minor changes in the *Net* in Fig. S1d. Given the opposite variations of *C* and *T*, the net contribution of convection, tilting and stretching, and diffusion in the stable LEV region is at an order of one, indicating a reasonable balance of vorticity transport during the steady state. This balance of vorticity transport can prove the feasibility of conducting a quantitative analysis within the LEV region, as well as our methodology to outline the LEV region.

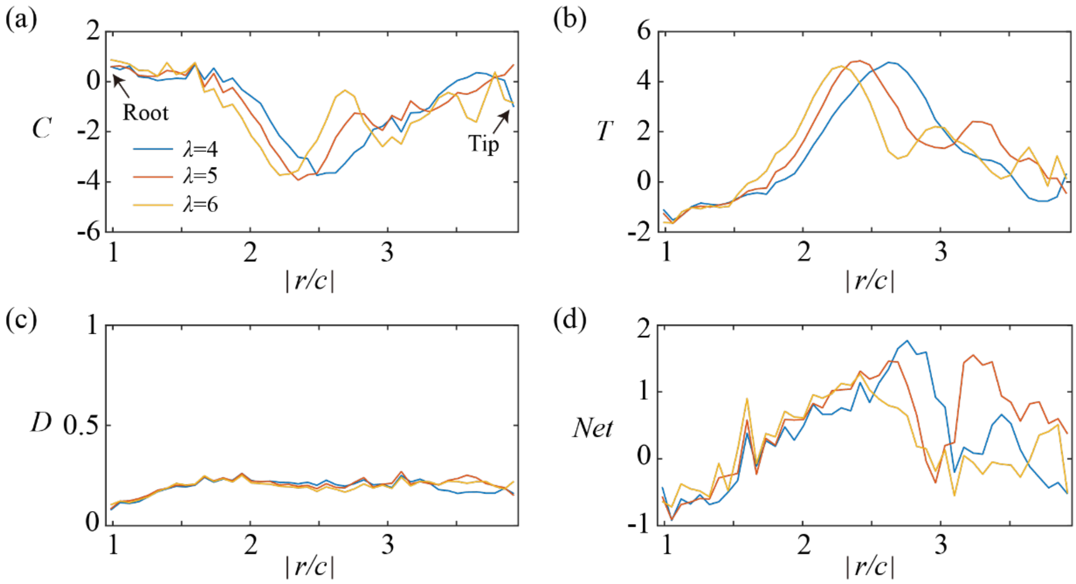

Fig. S1 Spanwise distribution of radial vorticity transport within the LEV region at the steady state of *Re*=1500. (a) total convection (*C*), (b) total vortex tilting and stretching (*T*), (C) total vorticity diffusion (D) and (d) net vorticity transport (*Net*=*C*+*T*+*D*). The LEV region is outlined by *Q*=1 and $\omega_r^* < 0$.

A sensitivity study is conducted to determine the threshold of *Q* (the second invariant of velocity gradient) in the integration of radial circulation described in Section 2.3. According to the definition, *Q*>0 infers that the local vorticity magnitude (i.e., rotation) is stronger than the local shear strain rate, thus indicating the formation of an ‘eddy’. It should be noted that a higher value of *Q* indicates an approaching towards the vortex core. In our sensitivity study, three *Q* values, i.e., 0.25, 1, and 2, are tested. As shown in Fig. S2, it is indicated that a higher *Q* threshold can shrink the LEV region and therefore results in a lower LEV circulation. However, the LEV circulation at *Q*=0.25 can be notably larger around the wingtip, especially at the steady state (Fig, S2b). This is because a smaller *Q* value can include the detached LEV into the integration. Therefore, the *Q*=1 threshold is chosen in the integration. This is also supported by the example shown in Fig. 3b (main text), where the *Q*=1 threshold can mostly delineate the strong vortical region and thus leading to a convincing result. Although a higher threshold of *Q* can limit the integration towards the LEV core, no qualitative variation of the integration is observed. Since our conclusions are based on a comparison of the relative strength of vorticity transport, the *Q*=1 threshold should be sufficient to avoid the inclusion of detached LEV while retaining most of the attached LEV.

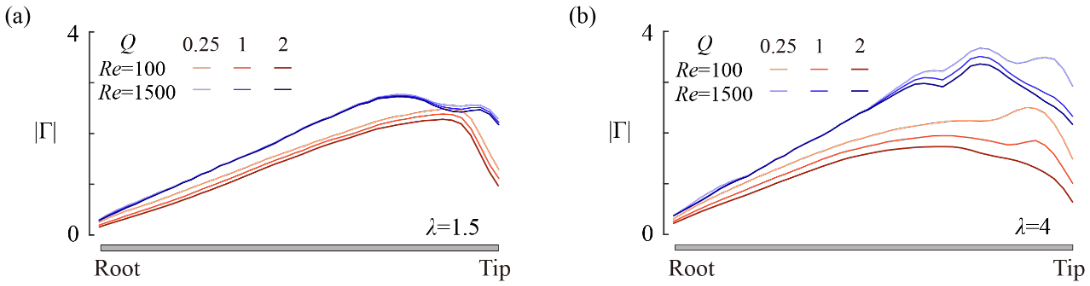

Fig. S2 Spanwise distribution of LEV circulation at different Q thresholds: (a) λ=1.5 and (b) λ=4.

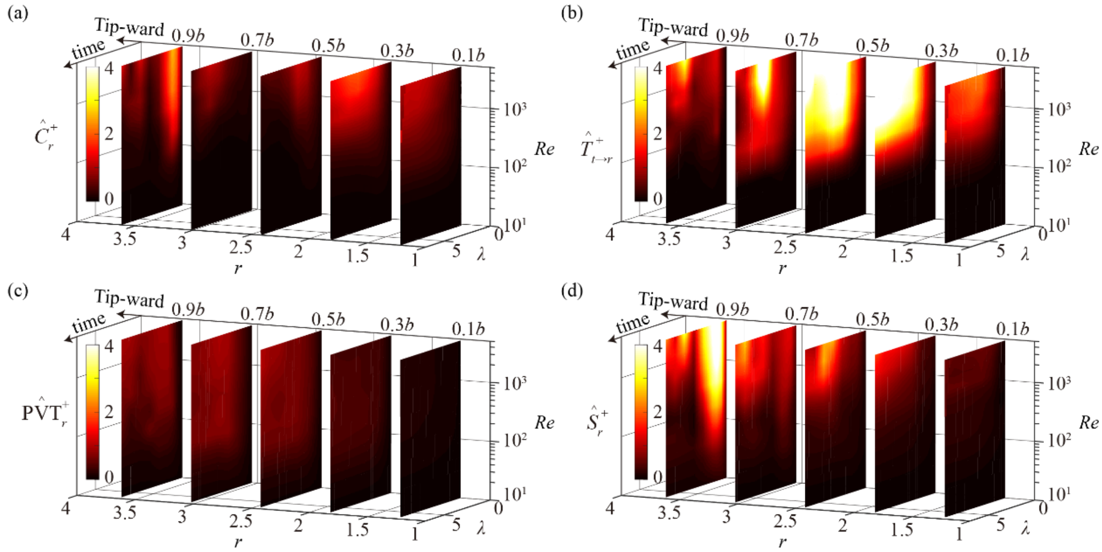

Fig. S3 Spatial-temporal variation of vorticity convection, vortex tilting and stretching that contribute to LEV stability. The threshold of Q is 0.25.

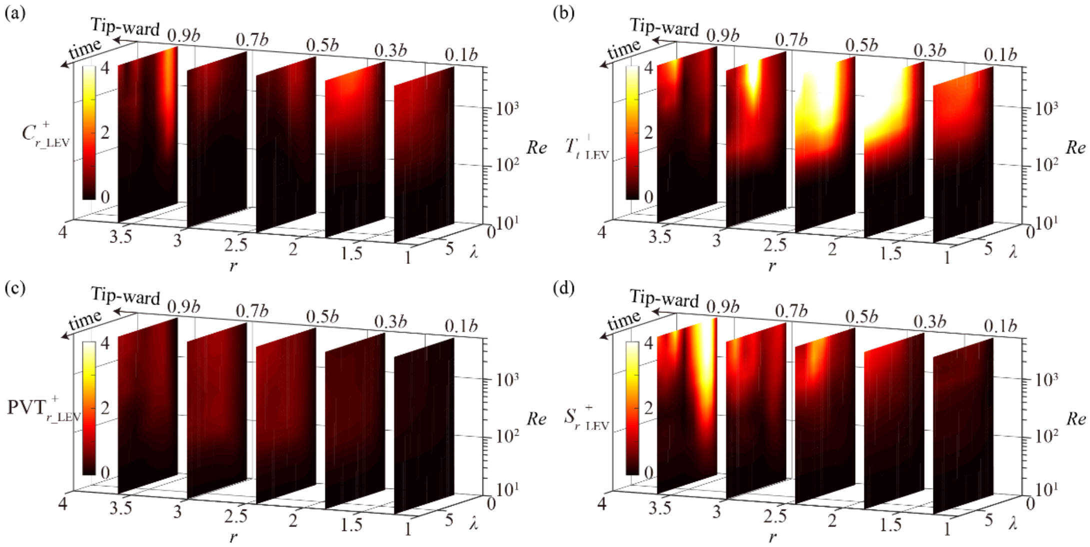

Fig. S4 Spatial-temporal variation of vorticity convection, vortex tilting and stretching that contribute to LEV stability. The threshold of Q is 1 (duplicated from Fig. 12 in the manuscript).

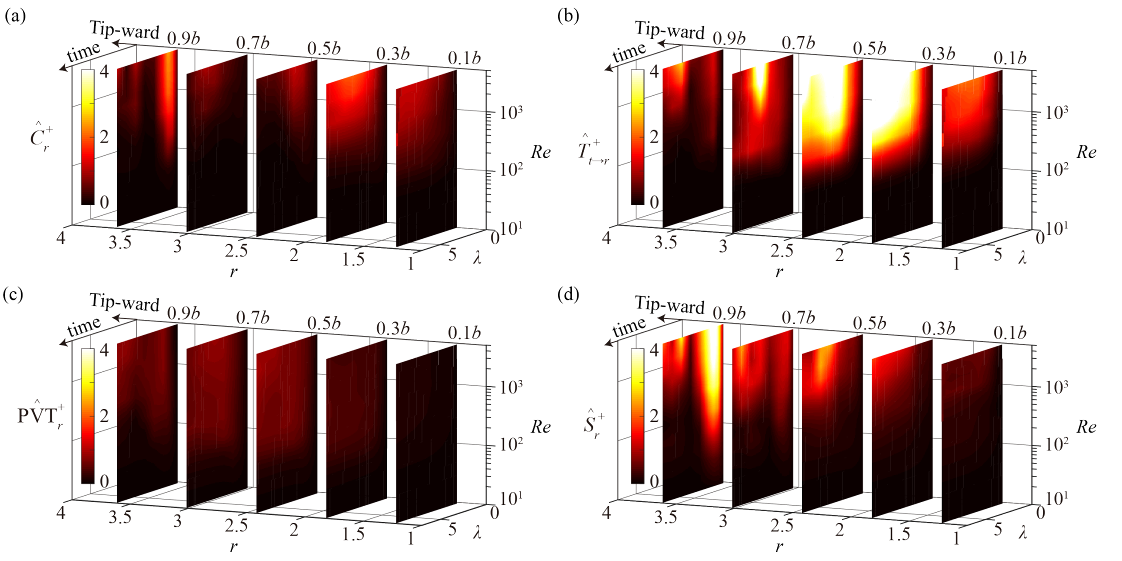

Fig. S5 Spatial-temporal variation of vorticity convection, vortex tilting and stretching that contribute to LEV stability. The threshold of Q is 2.

The feasibility of the Q=1 threshold is further supported by a comparison of the relative strength of critical vorticity convection, vortex tilting, and stretching (Figs. S3 to S5). As the Q threshold increases from 0.25 to 2, no qualitative difference is observed in the spatial-temporal variation of all four vorticity transport terms. The plots at Q=1 and 2 are almost identical, while the Q=0.25 threshold can lead to slightly higher integration of vorticity transport at 0.9b, e.g., $\hat{C}_r^+$ and $\hat{T}_{t\to r}^+$ in Fig. S3a. Therefore, the Q=1 threshold is applied in the integration.

The integrals of critical vorticity transport terms within the LEV can be expressed as a sum of their positive and negative sub-terms. Taking spanwise convection as an example,

$$\hat{C}_r = \hat{C}_r^+ + \hat{C}_r^- , \tag{1}$$

$$\hat{C}_r^+ = \int_{\mathrm{LEV}} C_r^{(+)} dS , \tag{2}$$

$$\hat{C}_r^- = \int_{\mathrm{LEV}} C_r^{(-)} dS . \tag{3}$$

Here, $\hat{C}_r^+$ and $\hat{C}_r^-$ are the integrals of positive and negative sub-terms of spanwise convection within the LEV region. Figures S6 and S7 present the spanwise distribution of these sub-terms of $\hat{C}_r$, $\hat{T}_{t\to r}$, $\mathrm{P\hat{V}T}_r$, and $\hat{S}_r$ at Re=1500 and 100. It is obvious that $\hat{T}_{t\to r}$ and $\mathrm{P\hat{V}T}_r$ are dominated by their positive sub-terms. However, both $\hat{C}_r$ and $\hat{S}_r$ experience a sign switching along the span. The LEV in the inboard region is mainly influenced by $\hat{C}_r^+$ (tip-ward convection, remove radial vorticity) and $\hat{S}_r^-$ (vortex stretching, enhance radial vorticity), whereas that in the outboard region is regulated by $\hat{C}_r^-$ and $\hat{S}_r^+$. Note that $\hat{S}_r$ becomes negligible at Re=100 and is thus removed from Fig. S7.

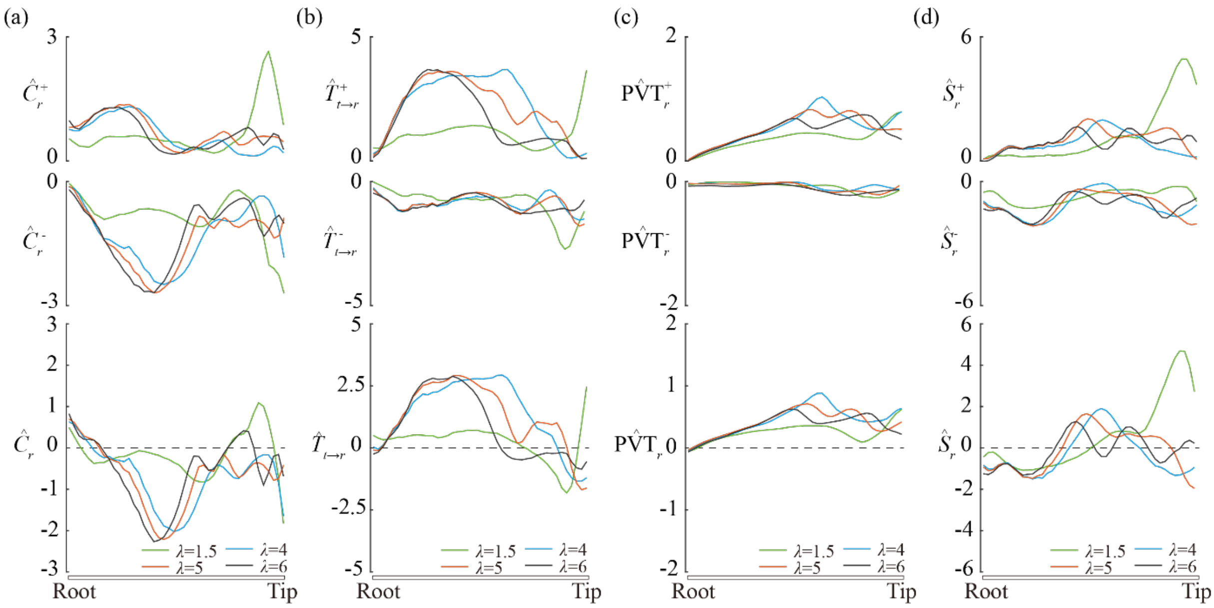

Fig. S6 Spanwise distribution of critical vorticity transport terms in the LEV at Re=1500: (a) C_r, (b) $T_{t\rightarrow r}$, (c) PVT_r, and (d) S_r.

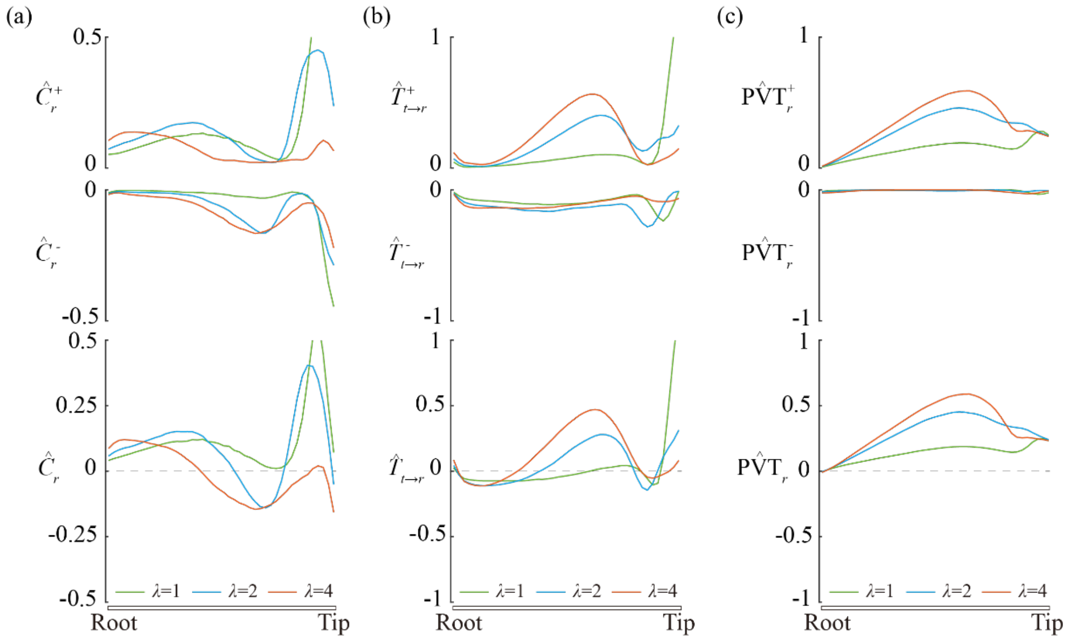

Fig. S7 Spanwise distribution of critical vorticity transport terms in the LEV at Re=100: (a) C_r, (b) $T_{t\rightarrow r}$, and (c) PVT_r.